Article

Flexible Photovoltaic System on Non-Conventional Surfaces: A Techno-Economic Analysis

Mostafa Esmaeili Shayan [1], Gholamhassan Najafi [1,*], Barat Ghobadian [1], Shiva Gorjian [1], Mohamed Mazlan [2,*], Mehdi Samami [3] and Alireza Shabanzadeh [3]

[1] Department of Biosystem Engineering, Tarbiat Modares University, Tehran 14115111, Iran;
    e.mostafa@modares.ac.ir (M.E.S.); ghobadian@modares.ac.ir (B.G.); gorjian@modares.ac.ir (S.G.)
[2] Advanced Material Research Cluster, Faculty of Bioengineering and Technology, University of Malaysia Kelantan,
    Jeli 17600, Malaysia
[3] Department of Electrical Engineering, Allameh Mohaddes Nouri University, Mazandaran 46415451, Iran;
    stu.samami@iausari.ac.ir (M.S.); alireza.shz@mohaddes.ac.ir (A.S.)
* Correspondence: g.najafi@modares.ac.ir (G.N.); mazlan.m@umk.edu.my (M.M.)

Abstract: Renewable energy policies emphasize both the utilization of renewable energy sources and the improvement of energy efficiency. Over the past decade, built-in photovoltaic (BIPV) technologies have mostly focused on using photovoltaic ideas and have been shown to aid buildings that partially meet their load as sustainable solar energy generating technologies. It is challenging to install conventional photovoltaic systems on curved facades. In this research, elastic solar panels assisted by flexible photovoltaic systems (FPVs) were developed, fabricated, and analyzed on a 1 m^2 scale. A flexible structure on a flat, hemispherical, and cylindrical substrate was studied in real terms. Using the LabVIEW application, warm and dry climate data has been recognized and transmitted online. The results showed that when installed on the silo and biogas interfaces, the fill factor was 88% and 84%, respectively. Annual energy production on the flat surface was 810 kWh, on the cylindrical surface was 960 kWh, and on the hemisphere surface was 1000 kWh, respectively. The economic results indicate that the net present value (NPV) at a flat surface is USD 697.52, with an internal rate of return (IRR) of 34.81% and a capital return term of 8.58 years. Cylindrical surfaces and hemispheres each see an increase of USD 955.18. The investment yield returned 39.29% and 40.47% for cylindrical and hemispheres structures. A 20% increase in fixed investment in the flat system increased IRR by 21.3%, while this increase was 25.59% in the cylindrical system and 24.58% in the hemisphere. Research innovation is filling the gap on the use of flexible solar panels on curved and unconventional surfaces.

Keywords: renewable energy; building integrated photovoltaic; sustainable; flexible photovoltaic systems; LabVIEW

1. Introduction

The Kyoto Protocol is an international agreement related to the United Nations on climate change, which requires countries worldwide to set specific carbon reduction targets around the world. The main concern of environmental policymakers is climate change mitigation. The impact of various factors on greenhouse gas (GHG) emissions has been studied by many authors [1]. Despite supply chain issues and construction delays caused by the pandemic, renewable capacity additions in 2020 increased by over 45% from 2019. Global wind capacity additions increased by 90%. Further underpinning this record growth was the 23% expansion of new solar photovoltaic (PV) installations to almost 135 GW in 2020 [2]. Utility-scale applications will account for about 70% of annual PV additions by 2022, up from 55% in 2020. Although China's significant feed-in tariff for commercial and industrial PV projects increased the ratio of distributed projects from 25% in 2016 to nearly 45% in 2018, this trend reversed in 2019 [3]. In the last decades, PV technology has

been drawing enormous attention worldwide. In the future, solar energy consumption is expected to increase due to further reductions in prices in solar cell technology [4,5]. Aside from the non-linear nature and environmental dependability of PV systems, the conversion of energy by PV panels is desirable [6]. It is a positive step towards obtaining energy from light through the advancement of science. Thanks to further cost reductions and continuous policy support from 120 governments globally, PV capacity additions are forecast to expand to 162 GW in 2022 [7,8]. Despite the ongoing COVID-19 pandemic, the overall investments in solar energy increased by 12% to USD 148.6 billion (EUR 125 billion). In 2020, over 135 GW of new solar photovoltaic electricity generation capacity was installed increasing the total cumulative installed capacity to over 770 GW [2]. The quality of electricity and the various sources of supply are now seen as the core solutions of policymakers around the world. Fossil fuels fall from almost four-fifths of total energy supply today to slightly over one-fifth [9]. Some of the most challenging environmental problems are the production and usage of oil resources and GHG. Every year, non-renewable energy releases a megatonne of GHG into the atmosphere [10,11]. In South Asia, the concept of using skin-based solar systems is on the rise. Building integrated photovoltaics (BPV) is increasingly used as a primary or secondary energy source in buildings. Unique criteria for the proper efficiency of the BPV cells need to be regarded. BPV is one of the most promising contributors to net-zero energy buildings, while also increasing the aesthetic value of the built environment and thermal and sound insulation properties [12]. The electrical power from the solar cells is increased by reducing the operating temperature; like all other semiconductor devices, solar cells are sensitive to temperature. Increases in temperature reduce the bandgap of a semiconductor which leads to the decrease of the module efficiency and output power [13,14]. Using natural or forced ventilation systems is one of the most effective ways to lower the solar cell temperature and increase efficiency. In addition, the solar system designer can position the solar cell in the direction of the wind at the correct position [15,16]. Iran's energy intensity index is up by a factor of 3. Developing countries can be expected to find themselves in a similar position. For developed countries, this index is about 0.3 [17]. Population growth and the need for energy usage, limitations and inability to react to refined petroleum products have increased the desire to use renewable energy, especially solar energy. Regardless of this, electricity demand per household has increased dramatically over 2007–2018 [18]. It is expected that this growth will occur until 2030 and that the slope will reach 60 percent [19]. In the supply of renewable energy and considered Iran's capacity, solar energy is environmentally sustainable, leading to non-CO_2 generation; it also contributes to natural resource sustainability, land recovery, reduced power transmission lines and cost-effectiveness of electricity transmission into rural areas [20]. Iran's Central Bank has reported that this sector's inflation rate was 10 percent a year based on the average inflation rate between 2011 and 2016 [21]. Research surveys have estimated that Tehran's sunny days and hours are about 313 days and 1742 h a year, respectively. The increase from the southeast to the northwest of Iran is reduced, whereas it usually increases from the west to the east [22]. The irradiance map and statistical irradiance simulations show that the irradiance level in clear air is theoretically high in Iran, including Yazd, Kerman, Tabas, Birjand, Iranshahr, Chabahar, Shiraz, Bam, Bushehr, and desert areas. However, building construction does not usually permit traditional solar systems with rigid modules [23]. The flexible solar cells can generate voltages of more than 50 V. These circuits will contain voltage appliances requiring higher setup power in the normal mode [24,25]. With a cumulative annual growth rate (CAGR) of the 200% compound, the cost of modules has declined from 260 cents/Wp in 2009 to 30 cents/Wp in 2018 [26]. The building's shape directly affects its energy use. Modern architecture regularly uses curved forms. They have a significant impact on the building's solar and energy performance, and may improve the internal environment. The curved shape is also used in silos, biogas tanks, greenhouses and structures. The Taguchi factorial experiment and response surface methods are used to improve the precision of the test and reduce the expense of testing and speed up the experiment [27]. Conventional solar panels involve the

construction of glass panels that are usually not quite consistent with cylindrical geometric shapes [28]. One of the solutions to these problems is the development and production of solar systems focused on flexible panels that are economical and provide the energy needs of the electrical equipment for curved structures [29]. Rural electrification in Iran was started by using photovoltaics in 2006, first in Qazvin province and then in Gilan, Zanjan, Bushehr, Yazd and Kurdistan provinces [30,31]. Hydrocarbons dominate Iran's energy mix. Traditional thermal power plants run on natural gas and petroleum derivatives such gasoline and fuel oil [32]. The remaining 2% comes from hydropower, nuclear, biofuels, and other renewables. Solar power plants have the least capacity of the three grid-connected power plants (wind, biogas, and solar) mounted [33]. Wind provides the majority of the renewable energy capacity [29,30]. Traditional houses in Iran are nearly zero energy buildings, which require local power generation to fulfill local energy consumption [34].

Flexible photovoltaic systems are suitable for buildings with complex shape envelopes, such as harvest silos, traditional islamic buildings, and petrochemical tanks. This critical phase can provide a portion of the electrical energy while preserving geometric and aerodynamic properties. The purpose of this study is to develop a flexible solar conversion system that can be used on curved surfaces to harvest sustainable renewable energy. We employed environmental evaluation and environmental strategies in this study to demonstrate the real potential of flexible solar energy conversion using pilot projects. This research has examined the technical and economic aspects of the knowledge gap of flexible solar panel technology for use at unusual surfaces and the cost of capital. The results of this analysis can expand the attractiveness of using this technology for historical and harmonic structures in the form of curves.

2. Materials and Methods

Flexible layers with suitable depth and durability can cover any design and introduce more incredible energy with selected columns. The current and voltage data collection was obtained by implementing the flat, cylindrical, and spherical surfaces. Figure 1 displays the analysis of specific traditional architectures under actual conditions. Rooftops and facades in the solar energy system are possible through software modeling and field testing. The structural part of the buildings was created in SketchUp, and the temperature analysis was performed in Ansys Workbench software. The components involved in the solar energy system were modeled in flat, cylindrical, and hemispherical shapes and studied under actual conditions. Data of irradiance, temperature, humidity and wind speed were recorded every 30 min through the data logger and sent to LabVIEW software via a USB-4711A device. A power meter measures and records the voltage, current, and output power of the systems. Throughout this process, the test layer was placed at 1 m^2, and the analysis and design of the radial and axial frameworks were taken out.

The solar power conversion model based on flexible panels, as shown in Figure 2 includes: geometric arrangement on cylindrical, hemispheric and flat surfaces, flexible solar cell, battery block, irradiance meter, temperature sensor, humidity sensor, anemometer, voltage monitor, power amplifier, planning circuits, battery plugs and fuses, analog-digital converter. The intensity of solar radiation was measured with a Multimetrix SPM72 Solar Meter with a maximum error of $\pm$5% (in the range of 0–1500 W/m^2 and $\pm$0.5 °C accuracy in the range of −10 to 110 °C), respectively. Moreover, the ambient temperature and surface temperature of solar cells were measured using 16 complete circuits of lm35 sensor connected to USB4711A with 0.1 °C accuracy and an Extech AN200 wind sensor with $\pm$5% accuracy in the wind speed range of 0.4 to 30 m/s.

Table 1 showed that flexible solar devices were used in agreement with the standards set out. Amorphous silicon (a-Si) element JNsolar3W-12v with three deposition junction points in a stainless polymer sheet and a lock diode were used to resist the leakage of the battery current to the solar module panel [35].
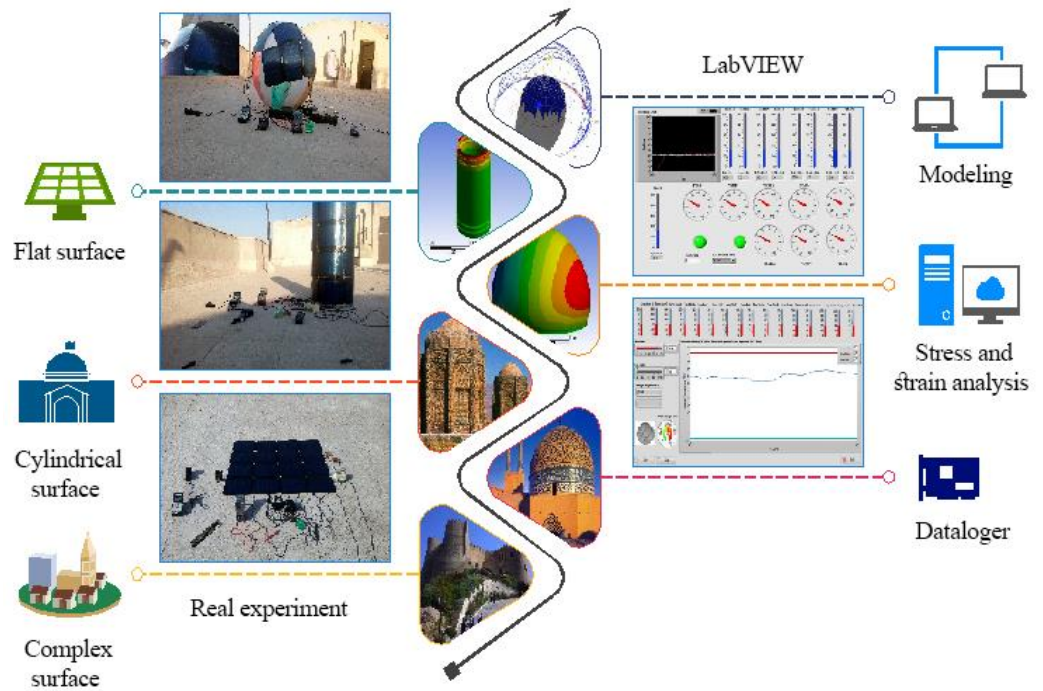
Figure 1. Flexible solar energy conversion system connected to LabVIEW software.

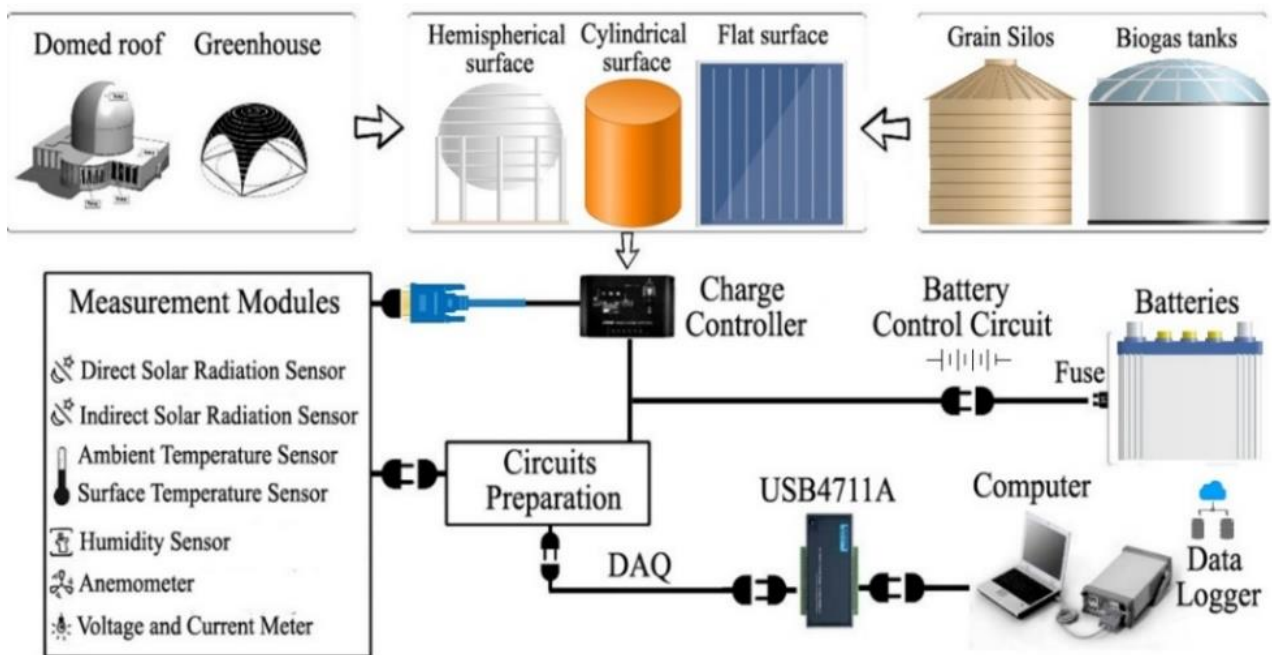**Figure 2.** Flexible solar system and monitoring devices.

Table 1. Specification of flexible solar module Jnsolar3w-12v [36].

Characteristic	Unit	Value
Power [1]	W	3.5
Short-circuit current	A	0.3
Absolute point voltage	V	12
Open circuit voltage	V	14
Dimensions	mm	(290,210,5)

[1] Power report in standard test conditions.

The most efficient matching layer provided by the choice of 1 m^2 solar panels could be 9744 cm^2. After removing the edges of the flexible solar panel, the photovoltaic section will be equal to 6996 cm^2. To cover the cylindrical and hemispherical surfaces with a specified area, 16 flexible solar elements, and a cylindrical and hemispherical structure with a particular area is required. A cylinder with a height of 84 cm and a radius of 18.5 cm, as well as a hemisphere with a radius of 39.38 cm, were designed and built for this purpose. Stress and strain analysis assisted in determining the space between the parts that would avoid damage. The structural models were created in SketchUp and the thermal stress analysis in Ansys Workbench showed a maximum strain of 0.041 mm in the radius direction. The strain was negligible, but to avoid rupturing the flexible parts, the contact distance was set at 2 mm. The maximum strain was 0.043 mm in the upper hemisphere. Therefore, a 2 mm contact distance was considered. As seen in Figure 1, the RS232 device and the LabVIEW software package were used to attach the temperature module. The microcontroller sends 16 temperature sensors per 50 milliseconds through a serial link and, until obtained by LabVIEW, shows them and stores them in an excel file per half-hour in a period. Fill factor (FF) is a parameter that, in conjunction with V_{oc} and I_{sc}, determines the maximum power from a solar cell. The FF is defined as the ratio of the maximum power from the solar cell to the product of V_{oc} and I_{sc}. The match principle is quantitatively similar to the current-voltage supply series, and the higher the amount, the greater the photovoltaic system's output. The FF is calculated on the surface according to Equation (1) [37,38]. The efficiency of a photovoltaic system is also one of the most critical external measurement items. Efficiency (η) is defined by Equation (2) [39].

$$FF = \frac{V_{MPP} \times I_{MPP}}{V_{oc} \times I_{sc}} \tag{1}$$

$$\eta = \frac{\frac{P}{S_t}}{G} \tag{2}$$

where G equals the irradiance (W/m^2), S_t equals the array layer (m^2), and P equals the device power at the target point (W). Excel 2019, Design Expert 7 and Minitab 18 were used in this study. Finally, the optimal power system was validated using the Taguchi test and response surface methodology (RSM).

Factorial design is used for a variety of tests. Taguchi can find the optimal point of operation of variables using a factorial design. Two variables, signal-to-noise (S/N) and ratio (η, dB), can determine the quality of experiment designed in Taguchi. A S/N ratio is a measure of robustness, which can be used to identify the control factor settings that minimize the effect of noise on the response. The S/N ratio is calculated for each factor level combination. The formula for the nominal-is-best S/N ratio using base 10 log is presented in the Equation (3) and the larger-is-better S/N ratio is shown in Equation (4) [40].

$$\frac{S}{N} = 10 \log\left(\frac{\bar{y}^2}{s_{\bar{y}}^2}\right) \tag{3}$$

$$\frac{S}{N} = -10 \log\left(\frac{1}{n} \sum_{i=1}^{n} \frac{1}{y^2}\right) \tag{4}$$

where n is the number of tests of the same level also with the goal of preserving the same S/N ratio at all times. The function level corresponding to the absolute average S/N ratio is considered the optimum level function. The expected value of the S/N ratio (η_{opt}) at the optimum parameter stage evaluated by Equation (5) is as follows [41]:

$$\eta_{opt} = \bar{n} + \sum_{i=1}^{k} (n_{mi} - \bar{n}) \tag{5}$$

where $\bar{n}$ is the mean S/N ratio of all experimental conditions, k is the number of critical parameters, and n_{mi} is the mean S/N ratio of the i th control factor corresponding to the optimal process point.

The test phase is divided into three parts: flat, cylindrical and spherical surfaces. Flexible solar panels are connected in series and off-grid from the mains with battery backup. Climatic data for the 27-day test was collected from the meteorological station and direct measurement instruments linked to the LabVIEW program. Table 2 shows the test factors and surfaces in the Taguchi and response surface methodology. For this test, four variables were chosen: irradiance, temperature, wind speed, and flexibility at three levels. The irradiance variable is rated from sunrise to sunset from 200 W/m^2 to 1100 W/m^2. The Taguchi test design and RSM method were analyzed based on maximum power generation capacity. Modeling in this work is evaluated based on the criterion "more power is better".

Table 2. Levels and responses of Taguchi and response surface methodology (RSM) design.

Factor	Variables	Units	Taguchi			RSM	
			Level 1	Level 2	Level 3	Low Actual	High Actual
A	Irradiance	W/m^2	200–500	500–800	800–1100	200	1100
B	Temperature	°C	20–30	30–40	40–50	20	50
C	Wind Speed	m/s	0–1	1–2	2–3	0	3
D	Flexibility	Degree	Flat	Cylinder	Hemisphere	0	π

The relationship between input and output values can be defined with x and y in energy systems design. A model can then be found in [41], where ε characterizes the noise or error reported in y output. Where the output results are:

$$y = f(x_1.x_2. \ \ldots \ .x_n) + \varepsilon \tag{6}$$

$$E(y) = (x_1.x_2. \ \ldots \ .x_n) = y \tag{7}$$

The Box–Behnken model design can include flat, cylindrical, and hemispheric surfaces. The model can be designed as follows in a flexible solar system:

$$\hat{y} = f(x_1.x_2. \ \ldots \ .x_n) \tag{8}$$

By analyzing the model's components, engineering economics will decide the rejection or acceptance of a project. COMFAR software has been used in this research, with the complexity of the system's economic variables and technological variables. The parameters used in the economic efficiency analysis for engineering economics are: net present value (NPV), benefit cost ratio (BCR), internal rate of return (IRR) and payback period (PBP). Maximum performance (electrical power generation) in watts is selected as statistical analysis.

3. Results and Discussion

This study investigates a flexible solar panel for energy on curved surfaces. We employed the actual capability of flexible solar energy conversion in this study, which was conducted utilizing environmental evaluation and environmental techniques centered on pilot projects. JNPsolar3W-12V flexible solar arrays generate flexible solar systems by fitting them to flat, cylindrical, and hemispheric base surfaces. The implemented model tested such systems theoretically and economically. The short-circuit current and the open-circuit voltage are the maximum current and voltage respectively from a solar cell. However, at both of these operating points, the power from the solar cell is zero. The shape of the I-V curve changes with the change in FF of the solar cell, which has been shown in Figure 3. By measuring the number of variances and its source of generation, the best output conditions were simultaneously predicted in systems, which is one of the advantages of using the Taguchi test method for solar energy systems. The minimum values of FF were calculated

as 0.73 for the flat surface and 0.88 and 0.84 for the cylindrical and hemispherical surfaces, respectively. The more significant FF for systems supports the power controller to take more voltage and power distribution.

The relationship of temperature, radiation and flexibility variables at the optimum level is studied in the proposed model. When the radiation is at level one, the device will begin to operate. Irradiance ranges between 400 W/m^2 and 600 W/m^2; then, the effectiveness is a little diminished, but it is still optimal for the system and satisfies the objective. More than 1000 W/m^2 of irradiance will have a negative impact on system performance. With an overall view of the irradiance power and the SNR band, it can be shown that irradiance intensity may substantially affect the function of the electrical power generation capacity through distancing itself from the center line and high failure.
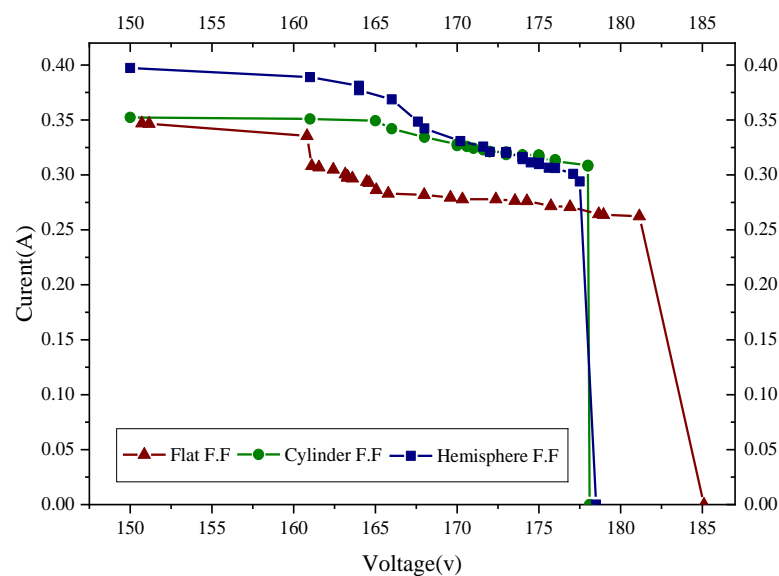
Figure 3. I-V curve modification with varying fill factor (FF).

The temperature in the latter group and the temperature level (3) had the most significant impact on the performance of the solar energy device. Incoming wind speed from level (1) to level (2) was useful for the subsystem and could change the conditions to produce power at extremely high temperatures. Flexibility or angles of the photovoltaic solar panels has shown that the change in this element, including the usage of the system in flat style (level 1) or when installed on a spherical surface (level 2) or on a cylindrical surface (level 3), may affect the production of the full power objective. The system angle group and the SNR revealed that level (1) defined as the flat surface layer might significantly affect the solar system. The application of the system at level (2), i.e., the application of the system to the spherical surface, considering its proximity to the middle power line goal, is more efficient than the levels (1) and (3). Level (3) indicated that the application of the method to a cylindrical surface is more efficient than a flat surface, but the optimum output is at level (2). The use of the process on the roof in flat styles, such as bitumen, is therefore not considered as the priority. When a system needs both grain silos and biogas reservoirs in a farm simultaneously, the operation of the device under these conditions would be superior to the hemisphere level, which implies the biogas reservoir.

The largest effect on the function of the flexible photovoltaic system, is related to the rate of irradiance, wind speed, temperature, and use on various PV shapes as flat, cylindrical and spherical materials. In the present experiment, Taguchi's study found that if the device were evaluated at chosen levels based on the optimal manufacturing process and variables, it would be possible to predict a combined power of 49.9 W with SNR = 33.929. If the function is measured separately and on a fully flat surface strength of the function, it would be equal to 53.3 W with SNR = 34.4918. When the model was used to calculate the

power on the cylindrical level, the device's power was equal to 54.05 W with SNR = 34.6368; for the hemispheric level, the corresponding power of 55.7 W with SNR = 34.8880. The choice of the hemispheric surface is then classified into first and second-level cylinder points. According to the Taguchi experiments, the dynamic conditions applied to the flexible solar system indicate the ideal conditions for the use of a flexible panel-based solar conversion system. Table 3 shows solar power production costs in different surfaces. Priority will therefore be given to the use of a solar energy conversion solution based on flexible solar panels at various stages, as described below.

- These systems have good performance in the range of 500 to 800 W/m^2. If the ambient temperature is between 20 and 30 °C, there will be no fall in performance due to the temperature on the cylindrical surface.
- For the next selection of the hemisphere's surface, it is best to have a consistent temperature, radiation, and wind speed parameters. The second level of radiation is 500–800 W/m^2, the first level of temperature is 20–30 °C, and the first level of wind is 0–1 m/s.
- The third choice for use of systems is for higher radiation up to more than 1000 W/m^2 in the middle of the day. This condition can occur in areas closer to the equator. The third level of radiation is 800–1100 W/m^2 and the first level of temperature is 20–30 °C, whereas the third level of wind is 2–3 m/s on the flat surface.

Table 3. List of solar power production costs in systems at different surfaces.

Systems	Power Production (kWh·USD)	Total Revenue Per Year (USD)
Flat	810.369 × 0.05	40.518
Cylinder	960.124 × 0.05	48.006
Hemispherical	1000.165 × 0.05	50.008

The cost (fixed price) of small-scale flexible photovoltaic panels is 0.8 USD/W. Therefore, 56 watts is equal to USD 44.8 in 2020. Thin-film technology has always been cheaper but less efficient than conventional c-Si technology. However, it has significantly improved over the years. In addition to the panel, other equipment is also used in the flexible photovoltaic systems. The total cost of a flexible photovoltaic system including the purchase of panels, installation costs, etc., is estimated at USD 181.78 according to the standard in current photovoltaic projects. Unforeseen costs included glue costs for reposing panels to surfaces, maintenance costs, and soil cleaning. The 20-year maintenance life of the solar system was estimated at USD 20 per year. Investment decisions are wracked with uncertainty and risk. Most investment models have explicit and implicit assumptions about the behaviors of models and the reliability and consistency of input data. If the changes made to the variables do not eliminate the project's justifiability, the investment will be much more favorable. In order to take into account factors not considered or the risk of agents endangering the return of the project, the sensitivity level of the project's indicators to these factors was estimated roughly. As seen in Figure 4, the irradiance peak is 1067.1 W/m^2.

In the cylinder, one side of the shadow and one side of the irradiance are usually present. For at least 3 h, the irradiance will be greater than 735 W/m^2. It is likewise at its peak in the middle of the day. At sunset, the irradiance will be at its lowest and will finally hit zero. After sunrise, the irradiance power on the south side of the test cylinder increased with a gentle slope, reaching a maximum of 1048 W/m^2 in the afternoon (around 14:00). These adjustments regulated the form of curved surfaces like the Sin type. Power for the hemisphere increased after sunrise and reached a maximum of 58.4 W at the beginning of the day. At midday (from 09:30 to 17:30), the power potential was almost constant at the hemispherical and cylindrical surface and was within the standard line range (55.5 W). Then, as the shade increases and the intensity of the light falls, the power decreases to zero.
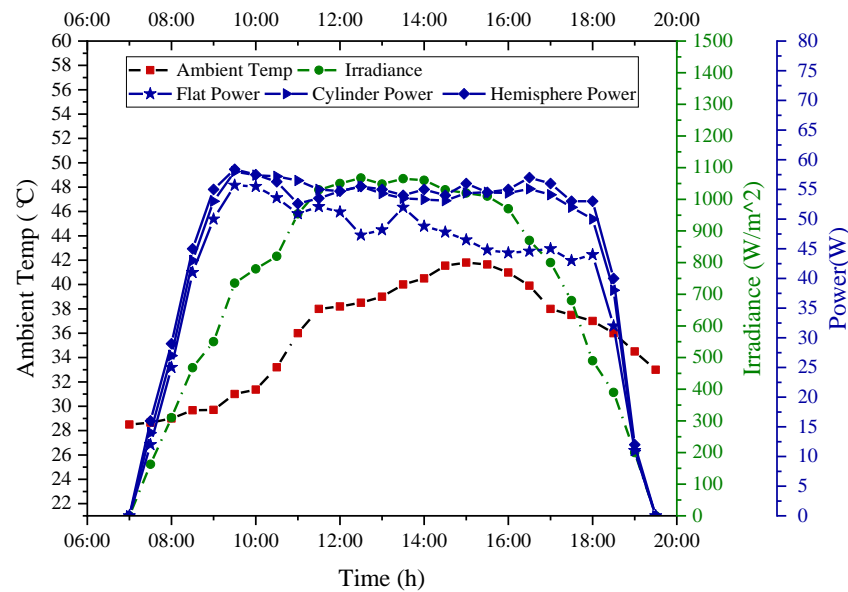
Figure 4. System factors and power analysis.

The maximum power (MP) in Taguchi test method is related to the system deployment on the cylinder facade and is equal to 59.87 W, while the minimum power of 57.84 W is related to the system when deployed on the flat surface. The maximum power in the RSM test is relevant to the system deployment on the hemispherical (H) surface and equal to 61.14 W, and the minimum power of system is 56.6 W when related to the extent on the flat surface. The system's performance (SP) under standard test conditions (STC) was measured to be 7.45%. The winter solstice occurs during the hemisphere's winter. In the Northern Hemisphere, this is the December solstice (usually December 21 or 22) and in the Southern Hemisphere, this is the June solstice (usually June 20 or 21). The minimum performance was measured at 7.09% and related to the flat surface. In the model analysis, the open-circuit voltage at the flat system level was equal to 185.7 volts, and the short-circuit current reached 0.347 A in the most optimum scenario. Furthermore, the maximum production current was 0.36 amps when the system was deployed on the hemispherical surface. Therefore, the system in the case of deployment on the hemispherical surface by receiving diffusion irradiances and vertical irradiances has optimal electrical and quality characteristics compared to other deployment surfaces. The second and third priorities are related to the cylindrical and flat surfaces, respectively.

Figure 5 shows the Pareto diagram. The effect of each variable on the output of the function in this figure is obvious. Pareto diagram Figure 5A is the highest rod on top of the graph and is related to the combined impact of variables; irradiance (A), humidity (C) and wind (E). This figure additionally describes the importance of combining relevant variables such as surface temperature (D), ambient temperature (B), radiation (A), wind (B), and humidity (C). In the fourth part, the mix of surface and wind temperature variables is vital. Additionally, analysis of free variables showed that the important power generation variables were surface temperature, radiation, ambient temperature, wind, and humidity.

Since radiation, surface temperature and ambient temperature variables are uncontrollable, the combined impact of radiation and temperature increase will reduce power generation. The system's response was at a level of 50 when installed on a flat surface: the use of flexible systems with a nominal output lower than the rigid photovoltaic systems has not achieved the desired efficiency and is not comparable with them. The impact of test factors on system power is shown in Figure 5B. The irradiance and wind speed factors have a positive effect on the system power, whereas the temperature factor has a negative impact. The optimum power in the cylindrical surface is 60.27 watts, once the ambient temperature is about 36 °C, radiation is 1050 W/m^2, the wind speed is zero, and the humidity is equal to 48.1%. Figure 6 shows the sensitivity analysis of systems. The sensitivity analysis figure

showed the impact of changing economic parameters by a variation of percentage (decrease or increase) on the IRR. This analysis showed changes in any of the parameters' estimated impact on the results of the evaluation. The most sensitive parameter is sales revenue on the flat surface, and then the increase in fixed assets has a more significant impact on IRR. In all three systems, solar energy sales revenue has the greatest impact on investment attractiveness and IRR. This factor has a nearly equal slope. The investment attractiveness and IRR share of the flexible photovoltaic system are related to its use on flat, cylindrical, and hemisphere surfaces, respectively. The increase in fixed assets of systems is the next factor that investors consider. Because of the long life of a flexible photovoltaic system and the low cost of maintenance and other costs, the operating cost factor plays a minor role in these systems' investment decisions.
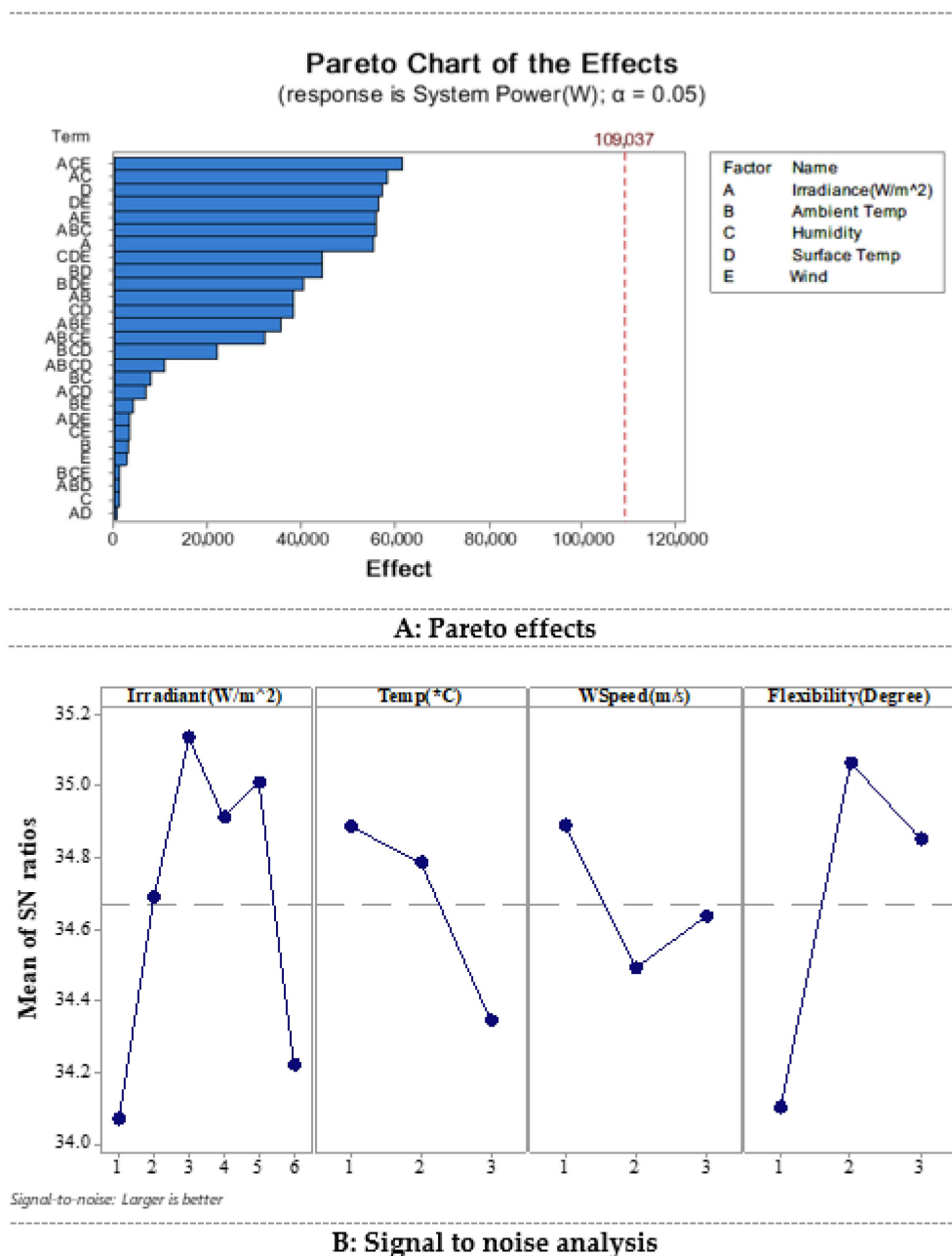

Figure 5. Effect of test variables on system power production quality in the actual test.
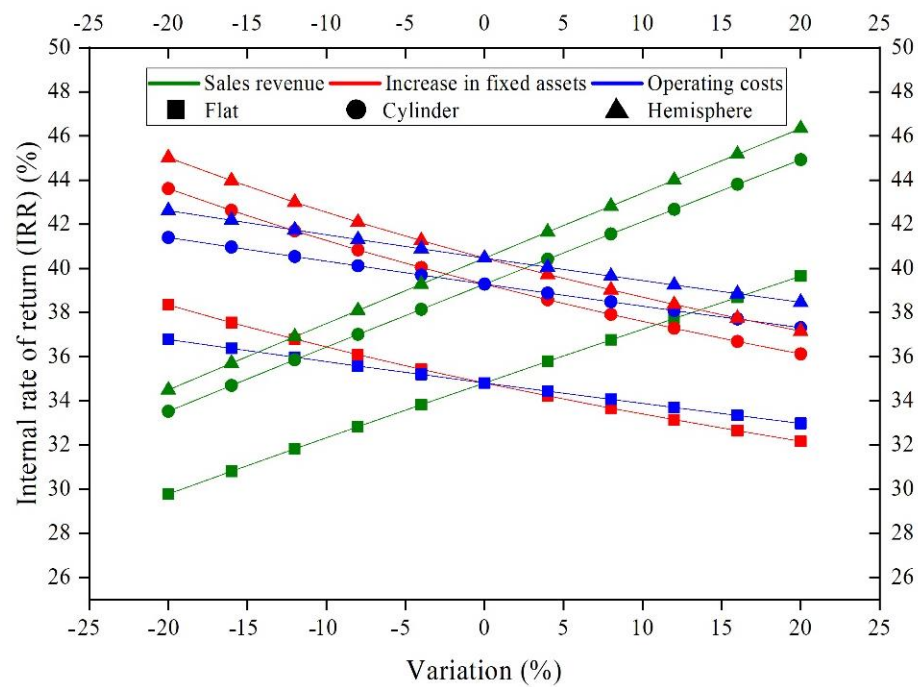
Figure 6. Effect of test variables on system power production quality in the actual test.

The economic findings show that the NPV of the flexible solar energy system at 16.70%, when applied at level (1), is USD 697.52, and that the IRR is 34.81% and the capital return duration is 8.58 years. This amount is increased to USD 900.88 in cylindrical surfaces and USD 955.18 in hemispheres. The rate of return on investment was 39.29% at the cylindrical level and 40.47% at the hemisphere. In the flat-surface production method, a 20% rise in project budget raised the internal yield by 21.3% and a 20% fall in sales. The project's internal rate of return would be reduced by 23%. Flexible solar systems installed on cylindrical and hemispheric surfaces experience a 20% rise in project prices, with the IRR rising by 25.59% and 24.48%, respectively. During the production time and deployment of flexible solar systems, the net flows were negative; when installed on cylindrical and hemispheric surfaces, from 7.20 years and 6.90 years to the end of the design period, the total net product flows were positive and constantly expanding. The description of the results is listed in the Table 4.

Table 4. Systems behavioral assessment for the 'more is best' target.

Power Plan	MP * Taguchi (W)	MP RSM (W)	FF (%)	P * (%)	OCV * (V)	SCC * (A)	IRR	NPV *
Flat S.	57.84	56.6	73	7.1	185	0.34	34.8	697.5
Cylindrical S.	59.87	57.71	88	7.4	179	0.35	39.2	900.8
Hemisphere S.	58.27	61.14	84	7.4	178	0.36	40.4	955.1

* MP = Maximum power; P = Performance; OCV = Open circuit voltage; NPV = Net present value.

4. Conclusions

Annual energy output was 810 kWh on a flat surface, 960 kWh on a cylindrical surface, and 1000 kWh on a hemisphere surface. Employing an optimum control approach based on the whale optimization method, reference [4] was able to enhance performance at the flat surface using solar power system upgrades, while the cylindrical and hemispherical surfaces were not supported by the system. In study [6], the fill factor was established as 78%, which we determined as 73% in our research, when maximum power point monitoring was used using the Taguchi approach for stand-alone photovoltaic systems. The cylindrical surfaces and hemispheres both obtained a USD 955.18 rise. Cylindrical constructions yielded 39.29% on investment, whereas hemispheric buildings returned 40.47%. In research [11],

the shading impact had a greater effect on the power of the photovoltaic system; however, in this study, the determining effects on the flexible photovoltaic system's electrical power generation, irradiance, temperature, and humidity were recorded. Although sources [12,13] claimed the optimum performance of the photovoltaic system at 1000 W/m², our study and [18,22,24] found that the ideal range for energy generation is consequently 800 W/m² in flexible photovoltaic systems. Economically, the current research system was estimated to cost USD 0.8 per watt, which is more costly than in other studies [26,27,29]. A reason for this is that equipment for gluing and mounting solar panels on cylindrical and hemispherical surfaces was used. The electrical performance of the solar system used in this research was 7.09%, which was less than 10% in comparison to organic photovoltaic [37] and triple junction flexible photovoltaic panels [39]. Electrical performance of 7.30% and 7.15% was recorded in these trials, respectively. The payback time varies by nation; in this research, it was computed at a flat rate of 8.25 years, although in other studies, it is often reported in the range of 3–5 years [4,15,27]. The pareto analysis introduces variables that affect system performance, but it is recommended to conduct on-site analysis of similar systems and compare the results during seasonal periods. It is proposed that modular systems be used in flags, towers, conventional structures, biogas tanks, grain storage silos, etc. It is preferable to install electrical systems on one side of the building, which has the largest average of shade. It is recommended that compact structures be used in regions similar to the equator and desert zones.

Recent research has sought to maximize the performance of solar power plants through the development of active materials and flexible substrates technology. With rapid progress development in recent years in new flexible photovoltaic material systems, such as organic semiconductors and metal halide perovskites, flexible PV panels are expected to be commercialized in many more future marketable products. Together with new generations of light energy storage devices, such as batteries and super capacitors, flexible solar cells are expected to be merged into many future mobile and flexible devices providing a renewable energy source for charging electronic equipment ranging from electric cars and electric bicycles, to smartphones and portable computers. Finally, the novel employment of wearable devices is investigated and reported to highlight the functionality of these practical platforms.

Author Contributions: Conceptualization, M.E.S. and G.N.; methodology, M.E.S.; software, B.G. and S.G.; validation, M.E.S., G.N. and M.M.; formal analysis, M.M. and A.S.; investigation, M.E.S.; resources, M.S.; data curation, S.G. and B.G.; writing—original draft preparation, M.E.S.; writing—review and editing, M.E.S. and G.N.; visualization, B.G and S.G.; supervision, M.E.S. and G.N.; project administration, M.E.S. and G.N.; funding acquisition, M.E.S. and G.N. All authors have read and agreed to the published version of the manuscript.

Institutional Review Board Statement: Not applicable.

Informed Consent Statement: Not applicable.

Data Availability Statement: Not applicable.

Conflicts of Interest: The authors declare no conflict of interest.

Nomenclature

Symbols		Greek Symbols	
A	Area (m²)	γ	Wind Speed (m·s⁻¹)
C_{cf}	Net Annual Cash Flow ($)	η	Efficiency (%)
CF_i	Cash Flow in the Time Period ($)	**Subscript**	
C_{inv}	Initial Investment ($)	mmp	Maximum Power Point
F	Flexibility (Degree)	sc	Short Circuit Current
FF	Fill Factor (%)	oc	Open Circuit Voltage

FiT	Feed in Tariff ($·kWh^{-1})	**Abbreviations**	
G	Irradiance (W·m^{-2})	a-Si	Amorphous Silicon
I	Current (A)	BCR	Benefit Cost Ratio
IRR	Internal Rate of Return (%)	BPV	Built Integrated Photovoltaic
NCF$_i$	Net Cash Flow for Period i ($)	BOS	Balance of System
NPV	Net Present Value ($)	c-Si	Crystalline Silicon
P	Power (W)	FPVs	Flexible Photovoltaic Systems
r	Discount Rate (%)	GHG	Greenhouse Gases
S$_t$	Array Layer (m^2)	PBP	Payback Period
S/N	Signal to Noise (dB)	PV	Photovoltaic
T	Temperature (°C)	RSM	Response Surface Methodology
t	Time (s)	SNR	Signal to Noise Ratio
V	Voltage (V)	STC	Standard Test Conditions

References

1. Liobikienė, G.; Butkus, M. Determinants of greenhouse gas emissions: A new multiplicative approach analysing the impact of energy efficiency, renewable energy, and sector mix. *J. Clean. Prod.* **2021**, *309*, 127233. [CrossRef]
2. Jäger-Waldau, A. Overview of the Global PV Industry. *Compr. Renew. Energy* **2022**, *1*, 130–143. [CrossRef]
3. IEA. Global Energy Review 2021—Analysis—IEA n.d. Available online: https://www.iea.org/reports/global-energy-review-2021 (accessed on 27 August 2021).
4. Hasanien, H.M. Performance improvement of photovoltaic power systems using an optimal control strategy based on whale optimization algorithm. *Electr. Power Syst. Res.* **2018**, *157*, 168–176. [CrossRef]
5. Yazid, M.N.A.W.M.; Sidik, N.A.C.; Mamat, R.; Najafi, G. A review of the impact of preparation on stability of carbon nanotube nanofluids. *Int. Commun. Heat Mass Transf.* **2016**, *78*, 253–263. [CrossRef]
6. Hong, Y.Y.; Beltran, A.A.; Paglinawan, A.C. A robust design of maximum power point tracking using Taguchi method for stand-alone PV system. *Appl. Energy* **2018**, *211*, 50–63. [CrossRef]
7. O'Shaughnessy, E.; Cruce, J.; Xu, K. Rethinking solar PV contracts in a world of increasing curtailment risk. *Energy Econ.* **2021**, *98*, 105264. [CrossRef]
8. Ettefaghi, E.; Ghobadian, B.; Rashidi, A.; Najafi, G.; Khoshtaghaza, M.H.; Rashtchi, M.; Sadeghian, S. A novel bio-nano emulsion fuel based on biodegradable nanoparticles to improve diesel engines performance and reduce exhaust emissions. *Renew. Energy* **2018**, *125*, 64–72. [CrossRef]
9. Najafi, G.; Ghobadian, B. LLK1694-wind energy resources and development in Iran. *Renew. Sustain. Energy Rev.* **2011**, *15*, 2719–2728. [CrossRef]
10. Awad, O.I.; Ali, O.M.; Mamat, R.; Abdullah, A.A.; Najafi, G.; Kamarulzaman, M.K.; Yusri, I.; Noor, M. Using fusel oil as a blend in gasoline to improve SI engine efficiencies: A comprehensive review. *Renew. Sustain. Energy Rev.* **2017**, *69*, 1232–1242. [CrossRef]
11. Chan, A.L.S. Effect of adjacent shading on the energy and environmental performance of photovoltaic glazing system in building application. *Energy* **2019**, *187*, 115939. [CrossRef]
12. Oduyemi, O.; Okoroh, M. Building performance modelling for sustainable building design. *Int. J. Sustain. Built Environ.* **2016**, *5*, 461–469. [CrossRef]
13. Zeb, R.; Salar, L.; Awan, U.; Zaman, K.; Shahbaz, M. Causal links between renewable energy, environmental degradation and economic growth in selected SAARC countries: Progress towards green economy. *Renew. Energy* **2014**, *71*, 123–132. [CrossRef]
14. Azadbakht, M.; Esmaeilzadeh, E.; Esmaeili-Shayan, M. Energy consumption during impact cutting of canola stalk as a function of moisture content and cutting height. *J. Saudi Soc. Agric. Sci.* **2015**, *14*, 147–152. [CrossRef]
15. Shukla, A.K.; Sudhakar, K.; Baredar, P.; Mamat, R. BIPV based sustainable building in South Asian countries. *Sol. Energy* **2018**, *170*, 1162–1170. [CrossRef]
16. Rabab Mudakkar, S.; Zaman, K.; Shakir, H.; Arif, M.; Naseem, I.; Naz, L. Determinants of energy consumption function in SAARC countries: Balancing the odds. *Renew. Sustain. Energy Rev.* **2013**, *28*, 566–574. [CrossRef]
17. Edalati, S.; Ameri, M.; Iranmanesh, M.; Tarmahi, H.; Gholampour, M. Technical and economic assessments of grid-connected photovoltaic power plants: Iran case study. *Energy* **2016**, *114*, 923–934. [CrossRef]
18. Al-Falahi, M.D.A.; Jayasinghe, S.D.G.; Enshaei, H. Hybrid algorithm for optimal operation of hybrid energy systems in electric ferries. *Energy* **2019**, *187*, 115923. [CrossRef]
19. Zohoori, M. Exploiting Renewable Energy Sources in Iran. *Interdiscip. J. Contemp. Res. Bus.* **2012**, *4*, 849–862.
20. Solangi, K.H.; Islam, M.R.; Saidur, R.; Rahim, N.A.; Fayaz, H. A review on global solar energy policy. *Renew. Sustain. Energy Rev.* **2011**, *15*, 2149–2163. [CrossRef]
21. Salehi-Isfahani, D.; Mostafavi-Dehzooei, M.H. Cash transfers and labor supply: Evidence from a large-scale program in Iran. *J. Dev. Econ.* **2018**, *135*, 349–367. [CrossRef]
22. Esmaeili Shayan, M. Solar Energy and Its Purpose in Net-Zero Energy Building. In *Zero-Energy Build—New Approaches and Technologies*; Pérez-Fargallo, A., Oropeza-Perez, I., Eds.; IntechOpen: London, UK, 2020. [CrossRef]

23.   Esmaeili Shayan, M.; Najafi, G.; Gorjian, S. *Design Principles and Applications of Solar Power Systems*, 1st ed.; ACECR Publication-Amirkabir University of Technology Branch: Tehran, Iran, 2020. (In Persian)

24.   Barr, M.C.; Rowehl, J.A.; Lunt, R.R.; Xu, J.; Wang, A.; Boyce, C.M.; Im, S.G.; Bulović, V.; Gleason, K.K. Direct Monolithic Integration of Organic Photovoltaic Circuits on Unmodified Paper. *Adv. Mater.* **2011**, *23*, 3500–3505. [CrossRef] [PubMed]

25.   Chen, J.E.J.; Kang, S.; Zhao, X.; Zhu, H.; Deng, Y.; Peng, Q.; Zhang, Z. Modeling and characterization of the mass transfer and thermal mechanics of the power lithium manganate battery under charging process. *Energy* **2019**, *187*, 115924. [CrossRef]

26.   Padmanathan, K.; Govindarajan, U.; Ramachandaramurthy, V.K.; Oli Selvi, T.S.; Jeevarathinam, B. Integrating solar photovoltaic energy conversion systems into industrial and commercial electrical energy utilization—A survey. *J. Ind. Inf. Integr.* **2018**, *10*, 39–54. [CrossRef]

27.   Dehghan, M.; Rahgozar, S.; Pourrajabian, A.; Aminy, M.; Halek, F.S. Techno-economic perspectives of the temperature management of photovoltaic (PV) power plants: A case-study in Iran. *Sustain. Energy Technol. Assess.* **2021**, *45*, 101133. [CrossRef]

28.   Keshtegar, B.; Mert, C.; Kisi, O. Comparison of four heuristic regression techniques in solar radiation modeling: Kriging method vs RSM, MARS and M5 model tree. *Renew. Sustain. Energy Rev.* **2018**, *81*, 330–341. [CrossRef]

29.   Ghritlahre, H.K.; Prasad, R.K. Application of ANN technique to predict the performance of solar collector systems—A review. *Renew. Sustain. Energy Rev.* **2018**, *84*, 75–88. [CrossRef]

30.   Esmaeili Shayan, M.; Ghasemzadeh, F. Nuclear Power Plant or Solar Power Plant. In *Nuclear Power Plants-Processes from Cradle to the Grave, Landon*; Awwad, N., Ed.; IntechOpen: London, UK, 2020. [CrossRef]

31.   Najafi, G.; Ghobadian, B.; Yusaf, T.; Rahimi, H. Combustion analysis of a CI engine performance using waste cooking biodiesel fuel with an artificial neural network aid. *Am. J. Appl. Sci.* **2007**, *4*, 756–764. [CrossRef]

32.   Mat Yasin, M.H.; Mamat, R.; Najafi, G.; Ali, O.M.; Yusop, A.F.; Ali, M.H. Potentials of palm oil as new feedstock oil for a global alternative fuel: A review. *Renew. Sustain. Energy Rev.* **2017**, *79*, 1034–1049. [CrossRef]

33.   Yin, Y.; Liu, T.; He, C. Day-ahead stochastic coordinated scheduling for thermal-hydro-wind-photovoltaic systems. *Energy* **2019**, *187*, 115944. [CrossRef]

34.   Mohammadi, M.; Ghasempour, R.; Razi Astaraei, F.; Ahmadi, E.; Aligholian, A.; Toopshekan, A. Optimal planning of renewable energy resource for a residential house considering economic and reliability criteria. *Int. J. Electr. Power Energy Syst.* **2018**, *96*, 261–273. [CrossRef]

35.   Bloem, J.J.J.; Lodi, C.; Cipriano, J.; Chemisana, D. An outdoor Test Reference Environment for double skin applications of Building Integrated PhotoVoltaic Systems. *Energy Build.* **2012**, *50*, 63–73. [CrossRef]

36.   JMP. JNP. JP Solar 2017. Available online: http://jpsolar.net (accessed on 15 February 2018).

37.   Yan, J.; Luo, G.; Xiao, B.; Wu, H.; He, Z.; Cao, Y. Origin of high fill factor in polymer solar cells from semiconducting polymer with moderate charge carrier mobility. *Org. Electron.* **2015**, *24*, 125–130. [CrossRef]

38.   Abdolbaqi, M.K.; Azmi, W.H.; Mamat, R.; Mohamed, N.M.Z.N.; Najafi, G. Experimental investigation of turbulent heat transfer by counter and co-swirling flow in a flat tube fitted with twin twisted tapes. *Int. Commun. Heat Mass Transf.* **2016**, *75*, 295–302. [CrossRef]

39.   Esmaeili Shayan, M.; Najafi, G.; Lorenzini, G. Phase change material mixed with chloride salt graphite foam infiltration for latent heat storage applications at higher temperatures and pressures. *Int. J. Energy Environ. Eng.* **2022**. [CrossRef]

40.   Esmaeili Shayan, M.; Najafi, G.; Ghobadian, B.; Gorjian, S.; Mazlan, M. Sustainable Design of a Near-Zero-Emissions Building Assisted by a Smart Hybrid Renewable Microgrid. *Int. J. Renew. Energy Dev.* **2022**, *11*, 471–480. [CrossRef]

41.   Schwab, B.; Lusztig, P. A Comparative Analysis of the Net Present Value and the Benefit-Cost Ratio as Measures of the Economic Desirability of Investments. *J. Financ.* **1969**, *24*, 507. [CrossRef]